10.2478/v10048-010-0025-3

MEASUREMENT SCIENCE REVIEW, Volume 10, No. 5, 2010

Measurement of Viscoelastic Properties of Condensed Matter using Magnetic Resonance Elastography

Marco L.H. Gruwel[1]*, Peter Latta[1,2], Brendon Matwiy[1], Uta Sboto-Frankenstein[1], Patricia Gervai[1] and Boguslaw Tomanek[1]

[1]NRC-CNRC Institute for Biodiagnostics, 435 Ellice Avenue, Winnipeg MB, R3B 1Y6 Canada
[2]Institute of Measurement Science, Slovak Academy of Sciences, Dúbravská cesta 9, 84104 Bratislava, Slovakia

Magnetic resonance elastography (MRE) is a phase contrast technique that provides a non-invasive means of evaluating the viscoelastic properties of soft condensed matter. This has a profound bio-medical significance as it allows for the virtual palpation of areas of the body usually not accessible to the hands of a medical practitioner, such as the brain. Applications of MRE are not restricted to bio-medical applications, however, the viscoelastic properties of pre-packaged food products can also non-invasively be determined. Here we describe the design and use of a modular MRE acoustic actuator that can be used for experiments ranging from the human brain to pre-packaged food products. The unique feature of the used actuator design is its simplicity and flexibility, which allows easy reconfiguration.

Keywords: MRI; non-invasive; brain; food products; shear stress; elasticity; acoustic waves.

1. Introduction

Both conventional magnetic resonance imaging (MRI) and computed tomography (CT) of condensed matter usually provide a small range of signal variation [1]. MRI can provide high soft tissue contrast based on the approximate one order of magnitude difference in spin relaxation properties while CT X-ray attenuation coefficients vary by a factor of two. In order to determine changes in tissue due to disease in medical applications, the invasive administration of contrast agents is thus often required to adequately distinguish normal and diseased tissue. Viscoelastic properties of soft biological tissue, on the other hand, can vary by more than two orders of magnitude [2]. Similar arguments apply to non-biological soft condensed matter such as food products. Tissue viscoelastic properties thus provide a better image contrast range. MR elastography incorporates material viscoelastic properties as a contrast mechanism in conventional MRI. MRE is a phase-contrast magnetic resonance imaging technique to map spatial displacement patterns corresponding to harmonic shear waves initiated by the mechanical oscillations of a specially designed actuator attached to the object [3, 4, 5]. Apart from the plethora of medical applications studying specific changes in tissue stiffness related to disease, *e.g.* liver fibrosis, cancer, *etc.* [6], MRE has also been used to non-invasively study phase transitions in gels [7].

Dynamic Mechanical Analysis (DMA) [8] and mechanical compression tests [9] are the recognized standard techniques to measure viscoelastic properties of condensed matter, *ex vivo*. Recently the use of a torsional resonator device for the measurement of the complex shear modulus was reported [10]. This device has the potential to be used *in vivo*, however, during surgery only. These invasive techniques do not provide information on spatial variations of the mechanical properties and only provide a bulk number. MRE on the other hand is capable of measuring spatial variations and can thus be used to demarcate tissue compositional changes, either due to disease in people or animals or due to the heterogeneous composition of food products.

Three common types of actuator designs are in use; electromagnetic, piezoelectric and pneumatic. The most commonly used is the electromagnetic actuator due to its simple and low-cost design. However, electromagnetic actuators can cause significant interference with the MR signal acquisition and often require special precautions. Piezoelectric actuators provide a strong force and an excellent control of motion frequency and magnitude. One drawback of this design is its higher complexity, price as well as problems with MR image distortions due to susceptibility and eddy current artifacts. The pneumatic-type actuator virtually eliminates these interference problems, however, the operating frequency range is usually limited to a range of up to 150 Hz.

In this paper we introduce an MRE acoustic actuator set-up that can be used for *in vivo* brain elastography measurements as well as for the measurement of viscoelasticity in food products and we show general applications.

2. Subjects and Methods

2.1. Actuators

A dual actuator driver and enclosure was constructed in order to increase actuator performance. A pair of standard active sub-woofers were used as a source of air pressure. At the center of the custom-built lids a hose connector was mounted to attach flexible tubing for the delivery of acoustic waves into the passive drivers (Fig. 1A). One of the sub-woofers

*Corresponding author: marco.gruwel@nrc-cnrc.gc.ca

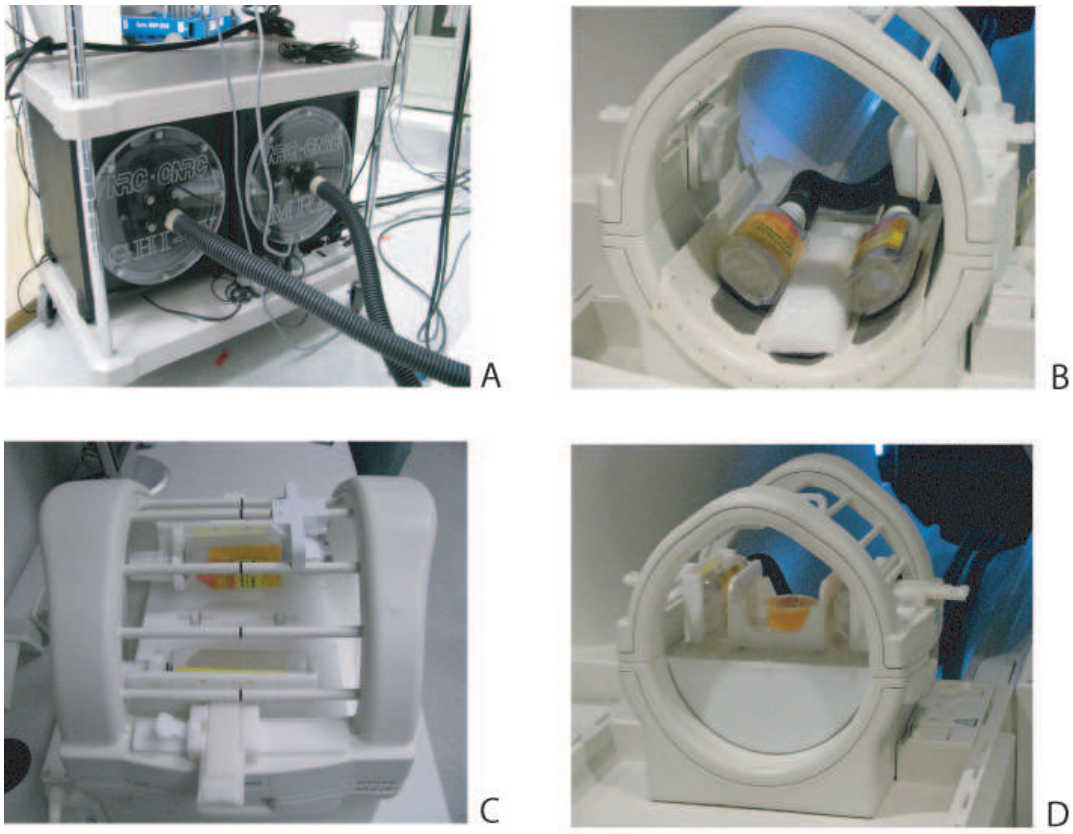

Fig. 1: A) Pair of modified active sub-woofers used to deliver the air pressure waves into the passive drivers. B) Head-type configuration with the actuators positioned at the bottom of the commercial RF-head coil. C,D) Bed-type configuration. In C) it is shown how the head-restrainers of the RF-coil have been replaced by the actuators. To accommodate the raised actuators, a table equipped with rollers has to be inserted into the coil, shown in D. In D), motion is induced from left to right, perpendicular to B_0.

was equipped with a switch to reverse the membrane motion and thus induce a mutual phase shift of 180° into the pressure waves generated from the speakers. The actuator concept is designed to operate with a standard transmit/receive head coil and for usage with three different configurations: head, probe and bed-type actuator. These configurations will be briefly described below.

- Head-type configuration: The driver unit consisted of standard polyethylene bottles (liquid honey bottles, noname™ brand). These containers have a flat rectangular shape with flexible walls, and can be placed in between the patient's head and the bottom of the RF-coil. A homemade fitting was used to connect the container to the hard-walled flexible tubes. The drivers are attached with Velcro® fasteners to a home-built plastic tray inserted into the bottom of the head coil (Fig. 1B).

- Probe-type configuration: For phantoms experiments using a small actuator contact area, the configuration can be changed to a so-called probe-type actuator. The passive drivers are placed in homemade brackets attached to the RF-coil in place of of the head restrainers. A T-bar with an actuator contact plate is positioned between the passive drivers and is secured with Velcro® strips. The height of the contact plate is adjustable using a screw. The contact plates are exchangeable according to the desired waveform shape.

- Bed-type configuration: When a large contact area with the source of oscillations is desirable, the configuration can be changed to a so-called bed type actuator. The passive drivers are placed in the brackets replacing the head restrainers in the same way as for the probe-type configuration. A table holder, equipped with four rollers, is positioned into the bottom part of the head coil. The rollers have glass ball bearings and their axes are positioned parallel to the main magnetic field, allowing motion in the direction perpendicular to B_0. The small cart positioned between the drivers serves as the sample holder (Fig. 1C,D). On the bottom of the cart, two notches were machined to keep it stable on the rollers during vibrations.

The frequency characteristics of all three actuator configurations have been examined in a bench test using a vibrationmeter(PCE-VT 2700, PCE Group, Meschede, Germany). The head-type configuration is operating most efficiently for fre-

quencies up to 80-90 Hz, where the motion amplitudes are $\sim$100 μm or more. However, a higher frequency range (up to 150 Hz) can be used for the bed-type and probe-type configurations.

2.2. Magnetic Resonance Experiments

All experiments were performed on a 3T medical scanner (TimTrio; Siemens Medical Solutions, Erlangen Germany) using a standard, single channel quadarature transmit/receive head coil. In order to eliminate any RF interference, the actuator driver and other electronics were placed outside the magnet room. Waveguide filters installed on the magnet shielding cage allowed for connections with equipment inside the magnet. An arbitrary function generator (Tektronix AFG3022B, Tektronix Inc. USA), triggered by the MRE pulse sequence was used to drive the acoustic oscillations generated by the sub-woofers. Homemade software written in LabVIEW (National Instruments, Corp, Austin, TX) was developed to setup waveform parameters. Synchronization and timing of the MRE experiments, *i.e.* trigger pulses, magnetic field gradients and the acoustic waveform was monitored using a 4-channel oscilloscope (BitScope BS-442N, Bitscope Designs, St. Leonards, NSW, Australia). Both the function generator and the Bitscope were controlled trough a local area network from a laptop computer placed inside the operator room.

The head actuator setup was used to collect *in vivo* data from the brains of healthy volunteers. Data sets with mechanical frequencies ranging from 50 to 90 Hz were acquired, while the volunteer was in the supine position. One motion encoding gradient (MEG) cycle of 32 mT·m^{-1} amplitude in the phase encode direction (parallel with anterior-posterior direction) was used to encode wave propagation at twenty different phase offsets within one wave cycle for the acoustic frequencies of 50 and 65 Hz. Three cycles of MEGs were use for the mechanical frequencies of 70 (see figure 2) and 90 Hz. MRE images of three axial slices with the center slice going through the genu and splenium of the corpus callosum were acquired with SE EPI, using the following parameters: repetition time (TR) of 6.0 s, echo time (TE) of 102 ms, a field of view (FOV) of 220^2 mm^2, a resolution of 128x128 pixels, a slice thickness of 5 mm and a fat saturation pulse was applied to suppress ghost artifacts from lipids. Over 10 healthy volunteers participated in the setup testing so far.

MRE experiments on food products were performed with the bed-type actuator configuration using a modified Gradient Echo sequence with a 40° RF-flip angle, an TE of 18 ms, a TR of 500 ms, a 10×10 cm^2 FOV, a 64×64 data matrix and sinusoidally shaped motion encoding gradients with strengths varying from 5 to 25 mT·m^{-1}. Motion encoding, using the oscillating sinus-shaped gradients, was performed at 75-150 Hz, to match the oscillation frequency of the sample. The number of motion encoding gradient pairs, using one cycle per acquisition, was set to 8, *i.e.* 8 images were acquired at a different phase of the oscillation. Prior to motion encoding the amplitude of the acoustic signal was ramped over a period of 200 ms to avoid transient signals [7].

Data processing was performed using MREwave, software obtained from Dr. Ehman's laboratory (Mayo Clinic, Rochester, MN). MREwave uses a local frequency estimation algorithm which provides an estimate of the local spatial frequency of shear wave propagation in the sample [11, 12]. The algorithm is relatively insensitive to phase noise and yields an accurate isotropic frequency estimation.

3. Theory

Most food products and biological materials, including living matter, can be considered viscoelastic materials due to their complex composition including biopolymers and water. Various models of viscoelastic behavior under stress or strain exists, however, biological materials are most often described using a linear model such as a Maxwell or Voigt model [13, 14]. The Maxwell model predicts a linear relation between strain and time which is not always observed while the Voigt model is not accurate in describing the relaxation after stress has been relieved.

Application of a sinusoidally modulated stress is known to result in a sinusoidally varying strain at the same frequency. This allows for the following definition of stress and strain in these materials:

$$\sigma = \sigma_0 \cdot exp(i\omega t) \tag{1}$$

$$\varepsilon = \varepsilon_0 \cdot exp(i(\omega t - \Delta\phi)) \tag{2}$$

Here σ represents stress while ε describes strain and $\Delta\phi$ the phase difference. The complex modulus describing their relation can thus be written as:

$$M(\omega) = \frac{\sigma_0}{\varepsilon_0} \cdot exp(i\Delta\phi) = M_1(\omega) + iM_2(\omega). \tag{3}$$

$M_1(\omega)$ is called the elastic (or storage) modulus, which is in phase with the applied oscillating strain, while $M_2(\omega)$ represents the viscous (or loss) modulus which is out of phase (90°) with the applied strain. For the Voigt model, these complex moduli are related to the elasticity modulus E, and the viscosity coefficient η, by:

$$M_1^V(\omega) = E \tag{4}$$

$$M_2^V(\omega) = \omega \cdot \eta \tag{5}$$

For the Maxwell model the moduli are defined as:

$$M_1^M(\omega) = \frac{E \cdot \omega^2\eta^2}{E^2 + \omega^2\eta^2} \tag{6}$$

$$M_2^M(\omega) = \frac{E^2 \cdot \omega\eta}{E^2 + \omega^2\eta^2} \tag{7}$$

Assuming we can describe the objects as isotropic homogeneous and incompressible systems, the propagation of shear waves can be modeled by the Helmholtz equation [13]. The Helmholtz equation allows us to calculate the shear speed attenuation for the Voigt and Maxwell model in terms of the

Lamé coefficients μ_l and η_s for shear elasticity and viscosity, respectively, as:

$$c_s^V(\omega) = \sqrt{\frac{2(\mu_l^2 + \omega^2\eta_s^2)}{\rho(\mu_l + \sqrt{\mu_l^2 + \omega^2\eta_s^2})}}, \quad (8)$$

$$c_s^M(\omega) = \sqrt{\frac{2\mu_l}{\rho\left(1 + \sqrt{1 + \frac{\mu_l^2}{\omega^2\eta_s^2}}\right)}} \quad (9)$$

Usually, for biological tissues and gels, the density, ρ, is assumed to be 1000 kg·m^{-3} as a very good approximation. For a pure elastic medium ($\eta = 0$) and according to the Voigt model, the speed of the shear waves becomes frequency independent. This can be considered the low-viscosity approximation. In this limit, the Maxwell model provides $c_s^M(\omega) \approx \sqrt{2\mu_l \cdot \rho^{-1} \cdot \omega\eta_s}$ which indicates a frequency dependence. For viscoelastic media the shear wave speed is predicted to increase monotonically with frequency for either model outside the low viscosity limit.

4. Results and Discussion

In Figure 2 a shear stiffness map of the brain of a volunteer is shown with the corresponding standard EPI image, in A and C respectively. Consistent with previous reports [15, 16] regions in the vicinity of the brain surface such as cortical grey matter, as well as the cerebrospinal fluid in the ventricles appear softer than regions of white matter and central brain parenchyma.

The lower mechanical frequencies exhibited a substantially higher displacement and a better penetration into the deep brain areas when compared to the higher frequency data sets (not shown). On the other hand, data acquired with higher mechanical excitation frequencies could provide better spatial resolution, especially when a wavelength sensitive reconstruction approach such as e.g. LFE is exploited [11].

Figure 3C shows an MRI scout image of the fruit pudding. MRE was performed at four different actuator frequencies using the bed-type configuration; 75, 100 (shown in figure 3A,B), 125 and 150 Hz, to study the frequency dependence of the shear modulus. The actuator vibrations moved the sample from left to right in figure 3 while the shear waves propagated from bottom to top. In Figure 3A and B a map of the calculated shear modulus and Local Frequency, respectively, are shown for an actuator frequency of 100 Hz and a MEG strength of 10 mT·m^{-1}. The area in between the inclusions, indicated by the dashed squares in Figure 3C, is characterized by a shear modulus of μ_l =0.75±0.15 kPa and a f_{LFE} = 96.2±6.5 Hz. This value for μ_l compares well with previously reported shear moduli for alginate gels [17]. Seaweed (alginate) is an important component of the fruit pudding.

Fitting the frequency dependence of the shear wave velocity in fruit pudding over the measured frequency range of 75-150 Hz to eqn. 8, we obtained μ_l= 0.61±0.02 kPa and η_s= 0.49±0.03 Pa·s. The density of the pudding was fixed at 1000 kg·m^{-3}. For the measured $c_s(\omega) < 1$ m·s^{-1} in the excitation frequency range of $75 \leq f \leq 150$ Hz, the Voigt model thus provides a good description of the viscoelastic properties of the material. Using dynamic compression, a separate measurement of the shear modulus in samples of the fruit pudding was performed in parallel (not shown). Extrapolation of the dynamic compression measurements to 100 Hz resulted in a shear modulus of 0.69 kPa. This is in good agreement with the value obtained from LFE of the MRE data.

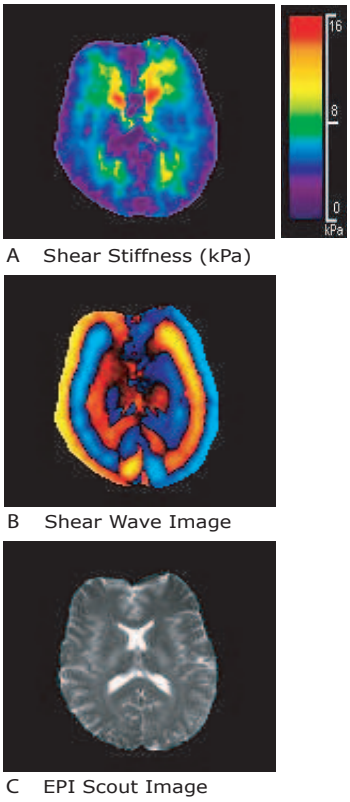

Fig. 2: A)The estimated shear stiffness map of the brain of a volunteer, calculated from the MRE phase images using the Local Frequency Estimation algorithm. The wave image is shown in B. The bottom figure C is that of an EPI scout image. The MEG direction was from bottom to top in the images. The actuators are positioned at the lower left and right hand bottom of the brain and were set 180° out of phase to induce a so called rocking-motion of 70 Hz.

All MRE data presented in this paper was processed using the LFE algorithm. This algorithm is relatively insensitive to noise, making it a perfect tool in combination with MR which sometimes can suffer from low signal to noise ratios. However, LFE suffers from limited resolution, causing blurring of the frequency estimate near sharp boundaries. As a result the estimation of the shear modulus suffers from errors at the edge of the sample or subject. For the same reasons inclusions and, more general for medical applications, cancerous or diseased

tissue, will have a blurred interfaced due to a rapid changing local stiffness. If the actual value of the shear modulus of inclusions, or diseased tissue is not of interest, the LFE is an excellent algorithm to detect these changes in local stiffness as they will be detectable as a change in local frequency (see Figure 3A).

Using the LFE algorithm thus allows for the accurate spatial detection of inclusions, however, not for the determination of their stiffness (in most cases, depending on the frequency used). Another algorithm, AIDE, based on algebraic inversion of the equations of motion (Helmholtz equation), requires the calculation of second derivatives which makes this algorithm very sensitive to noise and not so suitable for MR. So far these reconstruction models only considered attenuation due to elastic forces, however, recent attempts to include inertial forces in form a Rayleigh damping model have also been reported [18]. This approach might lead to a more detailed mechanism in differentiating soft tissue structures.

5. Conclusions

We have shown the application of MRE in two completely different fields of research using a convertible actuator design which allows for an easy and convenient setup of the various MRE measurements. Experiments with volunteers and food products showed that the actuator produces suitable shear waves, which can be used for the calculation of the elastic properties of soft condensed matter. The relation $c_s = \lambda \frac{\omega}{2\pi}$ and FOV of the MR image set a lower excitation frequency limit for the experiments while an upper limit is essentially set by the strength of the used encoding gradients.

6. Acknowledgements

The authors would like to thank Dr. Richard Ehman for introducing them to MRE using pneumatic actuators. Donghui Yin is thanked for his help with the construction of the actuator set-up. Drs. Valérie Pazos and Patricia Debergue are thanked for their help with the dynamic compression experiments.

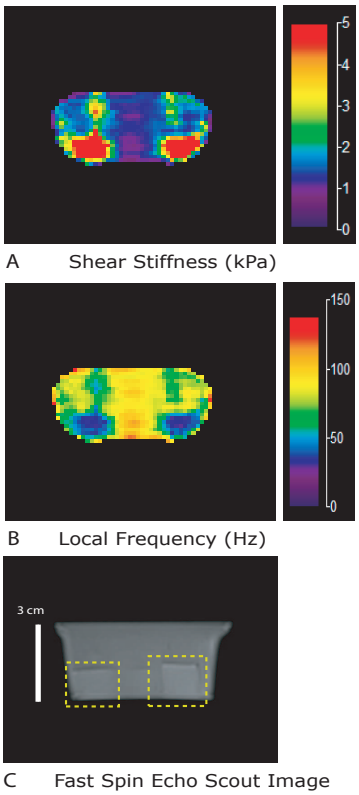

Fig. 3: The estimated shear stiffness (A) and local frequency (B), calculated from the MRE phase images using the Local Frequency Estimation algorithm. The bottom figure C is that of an MRI scout image clearly showing the chunks of coconut as indicated by the dashed squares. This slice orientation (5mm thick) was used for the MRE experiments. The coconut pieces can clearly be distinguished due to their different composition from the rest of the pudding. Note that the shear modulus between the two stiffer coconut inclusions appear rather homogeneous.

References

[1] Duck, F. A. (1990). *Physical Properties of Tissue*. Academic Press, San Diego, USA.

[2] Sarvazyan, A. (1993). Shear acoustic properties of soft biological tissues in medical diagnostics (a). *J. Acoust. Soc. Am.* 93, 2329–2330.

[3] Lewa, C. (1992). Mri response in the presence of mechanical waves, nmr frequency modulation, mechanical waves as nmr factor. *Acustica* 77, 43–45.

[4] Muthupillai, R., Lomas, D. J., Rossman, P. J., Greenleaf, J. F., Manduca, A., Ehman, R. L. (1995). Magnetic resonance elastography by direct visualization of propagating acoustic strain waves. *Science* 269(5232), 1854–1857.

[5] Plewes, D. B., Betty, I., Urchuk, S. N., Soutar, I. (1995). Visualizing tissue compliance with mr imaging. *J Magn Reson Imaging* 5(6), 733–738.

[6] Fatemi, M., Manduca, A., Greenleaf, J. F. (2003). Imaging elastic properties of biological tissues by low-frequency harmonic vibration. *Proceedings IEEE* 91(10), 1503–1519.

[7] Sack, I., Buntkowsky, G., Bernarding, J., Braun, J. (2001). Magnetic resonance elastography: a method for the noninvasive and spatially resolved observation of phase transitions in gels. *J Am Chem Soc* 123(44), 11087–11088.

[8] Jones, D. (1999). Dynamic analysis of polymeric systens of pharmaceutical and biomechanical significance. *Int. J. Pharmaceut.* 179, 167–178.

[9] Hamhaber, U., Grieshaber, F. A., Nagel, J. H., Klose, U. (2003). Comparison of quantitative shear wave mr-

elastography with mechanical compression tests. *Magn Reson Med* 49(1), 71–77.

[10] Valtorta, D., Mazza, E. (2005). Dynamic measurement of soft tissue viscoelastic properties with a torsional resonator device. *Med Image Anal* 9(5), 481–490.

[11] Oliphant, T. E., Manduca, A., Ehman, R. L., Greenleaf, J. F. (2001). Complex-valued stiffness reconstruction for magnetic resonance elastography by algebraic inversion of the differential equation. *Magn Reson Med* 45(2), 299–310.

[12] Knutsson, H., Westin, C., Granlund, G. (1994). Local multiscale frequency and bandwidth estimation. In: *Proc. ICIP-94. IEEE Int. Conf. Image Proces.* pp. 36–40.

[13] Steffe, J. (1996). *Rheological methods in food process engineering*. Freeman Press, East Lansing, MI, USA., 2nd edition.

[14] Catheline, S., Gennisson, J. L., Delon, G., Fink, M., Sinkus, R., Abouelkaram, S., Culioli, J. (2004). Measuring of viscoelastic properties of homogeneous soft solid using transient elastography: an inverse problem approach. *J Acoust Soc Am* 116(6), 3734–3741.

[15] Sack, I., Beierbach, B., Hamhaber, U., Klatt, D., Braun, J. (2008). Non-invasive measurement of brain viscoelasticity using magnetic resonance elastography. *NMR Biomed* 21(3), 265–271.

[16] Uffman, K., Maderwald, S., de Greiff, A., Ladd, M. (2004). Determination of gray and white matter elasticity with mr elastography. In: *Proc. Internatl. Soc. Magn. Reson. Med.*, Vol. 12. p. 1768.

[17] LeRoux, M., Guilak, F., Setton, L. (1999). Compressive and shear properties of alginate gel: effects of sodium ions and alginate concentration. *J. Biomed. Mat. Res.* 47, 46–53.

[18] McGarry, M. D. J., Houten, E. E. W. V. (2008). Use of a rayleigh damping model in elastography. *Med Biol Eng Comput* 46(8), 759–766.

Received September 29, 2010.
Accepted December 18, 2010.